

Star Forming Galaxies in the ‘Redshift Desert’

C. Steidel¹, A. Shapley², M. Pettini³, K. Adelberger⁴, D. Erb¹, N. Reddy¹, and M. Hunt¹

¹ California Institute of Technology, MS 105-24,
Pasadena, CA 91125, USA

² University of California, Berkeley

³ Institute of Astronomy, Cambridge, UK

⁴ Carnegie Observatories

Abstract. We describe results of optical and near-IR observations of a large spectroscopic sample of star-forming galaxies photometrically-selected to lie in the redshift range $1.4 \lesssim z \lesssim 2.5$, often called the “redshift desert” because of historical difficulty in obtaining spectroscopic redshifts in this range. We show that the former “redshift desert” is now very much open to observation.

1 Background

The “redshift desert” results from an accident of nature in which the windows of low atmospheric opacity and low terrestrial background are barren of familiar, strong spectroscopic features that make redshift identification easy using ground-based spectroscopy. At $z \sim 1.4$ the last of the strong nebular lines, [OII] $\lambda 3727$, passes well into the range where most optical spectrographs perform less well because of decreasing CCD quantum efficiency and rapidly increasing sky brightness. The result has been that there is a dearth of direct spectroscopic information on galaxies at $z \gtrsim 1.4$ until $z \gtrsim 2.5$, at which point (for star forming galaxies, at least) techniques like Lyman break selection coupled with normal optical spectroscopy have been quite successful. The difficulties with spectroscopy in the desert translate directly into larger uncertainties in photometric redshifts, since both methods depend on strong spectral features at observationally accessible wavelengths. Of course, nature has conspired to make this redshift range between $z \sim 1.5 - 2.5$ perhaps one of the most crucial in understanding the development of massive galaxies and of their central black holes, as we have heard from a number of talks at this meeting. There is thus a very strong impetus to gain access to galaxies in this range of redshifts, in spite of the difficulties that may be encountered.

Following the familiar rest-optical nebular lines into the near-IR is certainly possible in principle, but to date there has been little effort to do this in a wholesale manner because there have not been many instruments capable of multiplexed spectroscopy in the near-IR; this of course will change significantly over the next $\sim 3 - 5$ years as cryogenic multi-object near-IR spectrographs come on line. We have adopted an alternative strategy: to push faint object spectroscopy into the blue/UV portion of the observed spectrum, where the same spectral features used for the identification of galaxies at $z \sim 3$ [1] remain

accessible down to $z \sim 1.4$, thereby closing the gap in redshift space that has been called the “desert”.

Studying galaxies at $z \sim 2$ is quite rewarding for both scientific and practical reasons: This redshift range $1.5 \lesssim z \lesssim 2.5$ evidently contains the peak of the QSO epoch, and may well contain the formation era for most of the stars in today’s massive galaxies, judging by the redshift distribution of bright sub-mm sources [2]. But it is much more than a crucial epoch for galaxies and AGN—at these redshifts, it is possible to simultaneously study the diffuse intergalactic medium (IGM) *and* star forming galaxies in the same volumes, allowing for a direct examination of the magnitude of the effects of supernova feedback on the properties of galaxies and the IGM. Because both background QSOs and spectroscopically accessible galaxies have much higher surface densities than at higher redshifts where such experiments have already been done [3], $z \sim 2$ may be the optimal redshift for joint IGM/galaxy studies. In terms of attaining physical understanding of the galaxies one finds, $z \sim 2$ offers significant advantages as well: first, the surface density of galaxies bright enough for detailed spectroscopic studies using 8m-class telescopes at both optical and near-IR wavelengths is high; secondly, as we describe below, one has access to diagnostic spectroscopy in both the rest-frame far-UV *and* the rest-frame optical, allowing independent means of measuring physical properties such as chemical abundances, stellar initial mass function, and mass.

2 Survey of the “Redshift Desert”

We began our survey of $z \sim 2$ galaxies in the fall of 2000 just after the commissioning of the LRIS-B instrument (see [4]) on the Keck I telescope. Our approach to identifying which galaxies to target in order to efficiently survey galaxies at $z \sim 2$ was largely empirical, in the sense that we chose the region in color-space that would be occupied by galaxies having the same rest-frame SEDs as $z \sim 3$ LBGs in the sample of objects that have been observed from $0.3 - 2.2 \mu\text{m}$ (see [5] for a full description and motivation of the color selection). Generally speaking, this means that the galaxies we are selecting for spectroscopy have the same range of UV color as the better-studied LBGs at $z \sim 3$. Because we began our survey with the primary aim of studying the connection between the galaxies and the IGM, we have focused most of our efforts on the redshift range $2 \lesssim z \lesssim 2.5$ (we refer to this particular color selection as “BX” objects) where the Lyman α forest is easily studied from the ground, and in fields having more than 1 suitable $z \sim 2.5$ background QSO for studying the IGM component. However, we have recently obtained additional spectroscopy in both the GOODS-N and Groth/Westphal fields, where in addition to the $z \sim 2 - 2.5$ “BX” objects we have targeted objects expected to lie in the range $1.5 \lesssim z \lesssim 2$ (and which we refer to as “BM” objects). A more in-depth overview of the survey and its initial results is given in [4].

Figure 1 shows the results to date for the spectroscopy of the two new photometrically selected samples, with $\langle z \rangle = 2.20 \pm 0.32$ and $\langle z \rangle = 1.70 \pm 0.34$ for the

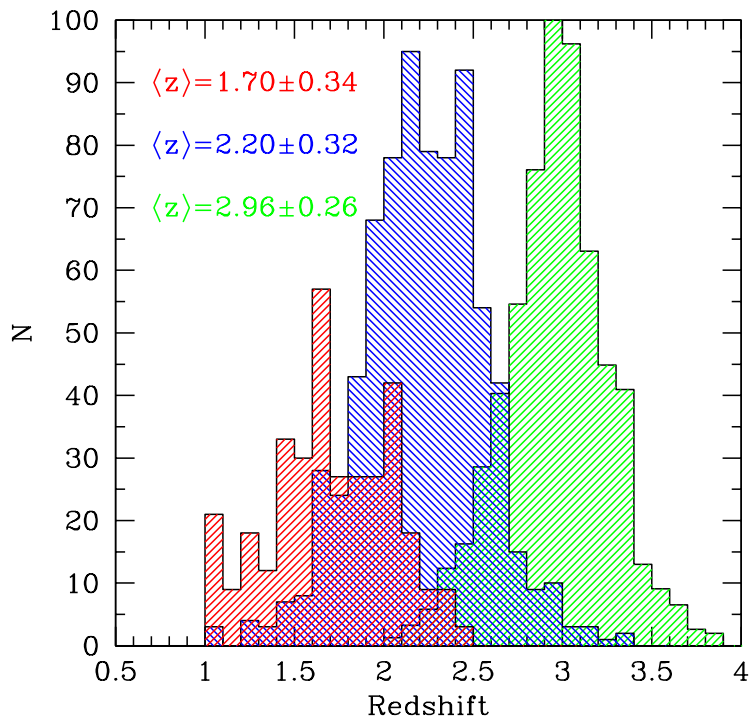


Fig. 1. Redshift histograms for rest-UV selected samples of star forming galaxies. The blue histogram is the 750 “BX” galaxies with spectroscopic redshifts at the time of this writing; the red histogram results from the “BM” selection targeting $z \simeq 1.5 - 2.0$ (118 redshifts, scaled by 3 for plotting). The green histogram is the $z \sim 3$ LBG sample of [1] (940 redshifts, scaled by 0.7 for plotting). The total number of new redshifts in the range $1.4 \leq z \leq 2.6$ is 792 at this time.

“BX” and “BM” samples, respectively. Figure 2 shows example LRIS-B spectra obtained since the science-grade detector system was installed in the instrument in June 2002.

The location of the $z = 1.5 - 2.5$ galaxies in color space (we use the same 3-band system used to isolate $z \sim 3$ galaxies) is easily estimated [5], and in fact galaxies in this range of redshifts are very common. After correcting for $\sim 8\%$ contamination by stars and low-redshift galaxies in the photometric samples, the total surface density of BX+BM galaxies is $\sim 9 \text{ arcmin}^{-2}$ to $\mathcal{R} = 25.5$ (our adopted spectroscopic limit), or about 25% of the number counts to the same apparent magnitude limit. With only 90-minute total integration times, the LRIS-B spectroscopy achieves $\sim 70\%$ success in identifying redshifts, primarily based on numerous interstellar absorption lines, as illustrated in Figure 2. Because LRIS-B is so efficient in the UV-visual range, and the sky is extremely dark, it is possible to collect high quality continuum spectroscopy in very reasonable integration times, so that the detection of strong emission lines

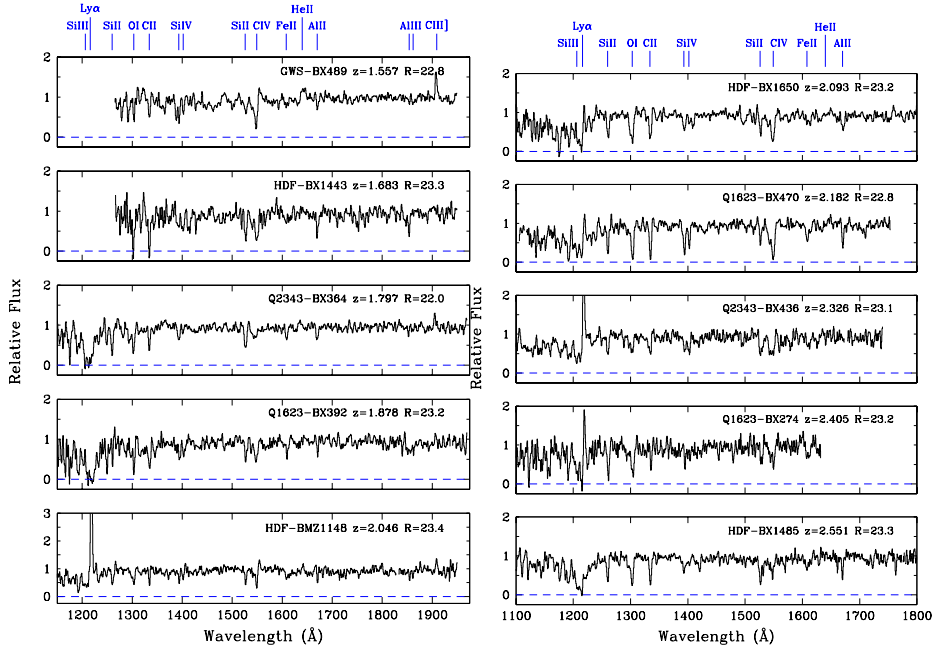


Fig. 2. Example LRIS-B spectra (shifted into the rest frame, but generally covering the wavelength range $3200 - 6000\text{\AA}$) of galaxies in the BX/BM sample covering the full range of redshifts and spectral properties seen in the sample. All spectra were obtained with 90-minute total integration times, in survey mode. The spectral resolution is $\sim 1.5 - 2.0\text{\AA}$ in the rest frame.

is completely unnecessary for achieving high spectroscopic completeness. At the time of this writing, we have obtained a total of more than 790 spectroscopic redshifts in the range $1.4 \lesssim z \lesssim 2.6$, with the distributions as shown in Figure 1. We have had similar success using LRIS-B to obtain spectra of objects which failed to yield redshifts in the DEEP2 redshift survey (see Jeff Newman’s contribution to these proceedings), where because of the spectroscopic configuration used, it is difficult to measure redshifts at $z > 1.4$. In general, LRIS-B is ideal for measuring redshifts for just the objects that generally fail to yield redshifts for spectroscopic setups focused on the red part of the optical spectrum.

3 Near-IR Observations of Optically Selected Desert Galaxies

3.1 Imaging

It is interesting to investigate the rest-frame optical properties of the rest-UV-selected “desert” galaxy population, particularly as a means of comparing them

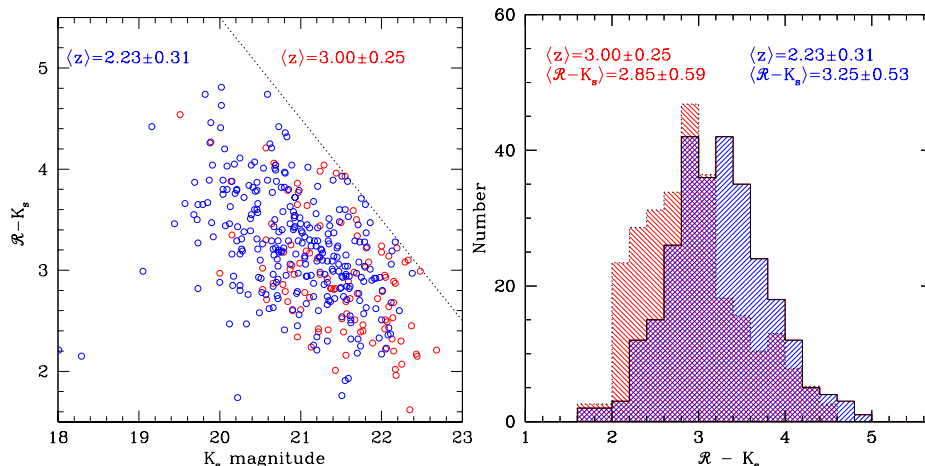


Fig. 3. Left: Color/magnitude diagram showing the 283 $z \sim 2$ galaxies with K -band measurements in our spectroscopic sample (blue points). The red points are taken from the $z \sim 3$ sample of [6]. The dotted line corresponds to our spectroscopic limit (for both surveys) of $\mathcal{R} = 25.5$. **Right:** Histograms of optical/IR color for the two samples, normalized to the same numbers. The $z \sim 2$ sample has many more galaxies with $(\mathcal{R} - K_s \gtrsim 3.2)$, which tend to be objects with significant Balmer breaks indicating extended star formation histories.

differentially to the similarly-selected $z \sim 3$ sample, and to various other surveys that use near-IR selection (e.g., FIRES, K20, GDDS—see contributions from Labbé, Cimatti, and Chen in these proceedings, respectively). Beginning in June 2003, with the commissioning of the Wide Field Infrared Camera (WIRC) on the Palomar 5m telescope, we have been obtaining very deep near-IR images of the regions of our survey fields with the densest spectroscopic coverage. In the first 3 pointings of the camera, which has a field of view of 8.7×8.7 arcmin, we have obtained K_s band measurements for a total of 283 ‘BX’ galaxies that already have spectroscopic redshifts. Although it requires very long (~ 12 hour) integrations on a 5m telescope, we have been able to reach limiting magnitudes of $K \sim 22.3$, allowing us to detect $\sim 85\%$ of the galaxies with spectra that fall within each pointing. Figure 3 shows a color-magnitude diagram of the 283 detected galaxies in the current sample. About 8% of these galaxies have $K_s < 20$ (the limit for the K20 survey) and $\sim 30\%$ has $K_s < 20.6$ (the limit for the Gemini Deep Deep Survey).

A cursory comparison of the distribution of $\mathcal{R} - K_s$ colors of the samples of star forming galaxies at $z \sim 3$ and $z \sim 2$ indicates that the $z \sim 2$ galaxies are significantly redder. Since objects with identical star formation histories observed at $z \sim 3$ and $z \sim 2$ are predicted to have essentially identical $\mathcal{R} - K_s$ color, the result suggests a real difference in the rest-optical properties of objects selected using the same rest-UV criteria in the two redshift intervals. The most likely cause of this is an increase in the average stellar mass of star forming galaxies at

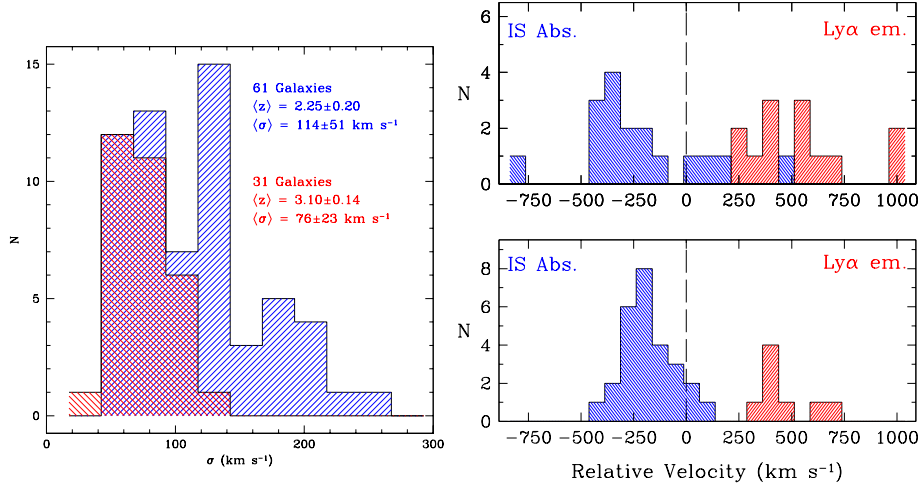


Fig. 4. Left: A comparison of the distribution of one-dimensional velocity dispersions (as measured using H α or [OIII] lines) for a sample of LBGs at $z \sim 3$ [8] (red) and $z \sim 2$ (blue). More than 50% of the $z \sim 2$ galaxies have σ larger than the largest values observed at $z \sim 3$. **Right:** a comparison of the galactic outflow kinematics of $z \sim 2$ (bottom) and $z \sim 3$ (top, [8]) galaxies.

$z \sim 2$ compared to their counterparts at $z \sim 3$. These results will be quantified in future work.

3.2 Spectroscopy

Galaxies at $z \sim 2$, and especially those at redshifts $z = 2 - 2.5$, are extremely well-suited for follow-up spectroscopy in the near-IR because the various nebular lines fall at favorable redshifts with respect to the atmospheric J, H, and K band windows. Using primarily the NIRSPEC instrument on the Keck II telescope, we have focused on observing the H α line primarily in the K-band window (initial results are presented in [7] and in the poster paper presented by Dawn Erb at this meeting). The scientific aims of these observations are manifold, and include 1) accurate measurement of the galaxy systemic redshift, crucial for analysis of the galaxy/IGM interface and for evaluating the velocities of supernova-driven outflows in the galaxies 2) measurement of the galaxy kinematics (line widths, rotation curves, etc.) 3) measuring chemical abundances in the galaxy's HII regions using various nebular line diagnostics and 4) additional estimates of star formation rates in the galaxies, possibly less affected by extinction than estimates based on UV continuum measurements.

Here we focus on the kinematics and chemical abundances. Our first observations ([7]) showed that the H α measurements could be made with a high success rate for the UV-selected $z \sim 2$ galaxies, and that in a reasonably high fraction of the cases observed, spatially resolved velocity shear was observed,

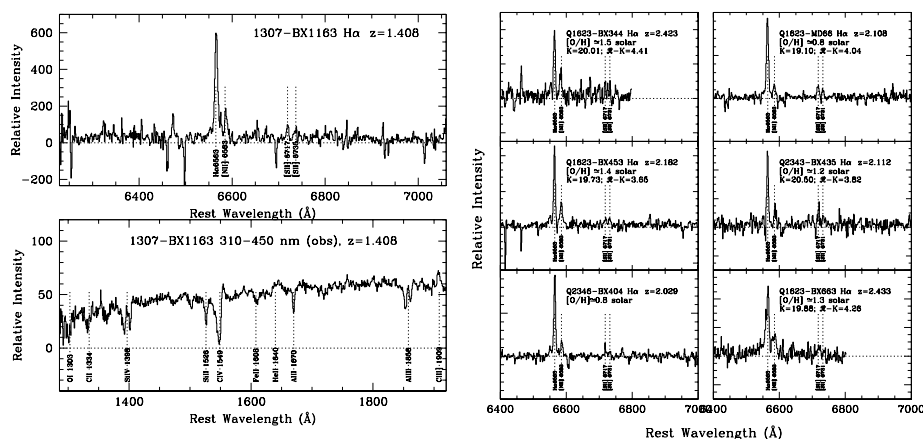


Fig. 5. **Left:** LRIS-B (lower) and NIRSPEC (upper) spectra of a galaxy at $z = 1.41$ illustrating the type of data from which detailed astrophysical properties of “desert” galaxies can be extracted. **Right:** Example NIRSPEC spectra of near-IR bright galaxies drawn from our UV-selected sample at $z \sim 2$. Using the calibration of [10] these have oxygen abundances that are consistent with being solar or greater.

such as might be expected in the case of rotating disks. The observability of such velocity shear in high redshift galaxies is very seeing dependent [9] but the overall line widths (σ) are also consistently larger than for the $z \sim 3$ galaxies in the sample of [8] despite the fact that they were selected on very similar UV properties. Comparisons of the $z \sim 2$ and $z \sim 3$ samples are shown in Figure 4—note that at $z \sim 2$, the line widths are much larger, while the galactic outflow kinematics, characterized by the velocities of the interstellar absorption lines and Lyman α emission with respect to the $H\alpha$ -defined redshift, are quite similar to the $z \sim 3$ counterparts. The most straightforward interpretation of both the 1-d line widths and the K_s band properties (§3.1) is that the stellar masses of UV-selected galaxies have increased considerably between the epochs corresponding to $z \sim 3$ and $z \sim 2$.

We have begun a program to obtain data suitable for measuring chemical abundances in the $z \sim 2$ galaxies, using both nebular indicators such as the $[\text{NII}]/H\alpha$ ratio ([10]) and also the rest far-UV features recorded in the optical LRIS-B spectra (see, e.g., Fig. 5a). Such observations allow significant insight into the physical nature of the galaxies: for example, from the spectra in Fig. 5a, we can infer [4] that both the nebular lines and the far-UV measurements indicate \simeq solar abundances, that the high mass end of the IMF is consistent with Salpeter, that the velocity dispersion of the HII regions of the galaxy is $\sigma = 126 \text{ km s}^{-1}$, and that interstellar absorption lines due to outflowing gas are blue-shifted by a bulk velocity of $\simeq 300 \text{ km s}^{-1}$ and have a velocity width of 650 km s^{-1} . In figure 5b, we show $H\alpha/[\text{NII}]$ spectra of objects selected to be

either bright in the K_s band or red in $\mathcal{R} - K_s$; for these objects, which comprise a significant fraction of the UV-selected sample, there are indications that the galaxies are typically solar metallicity or greater, even at $z \sim 2$; the full results of such analysis will be presented in [11].

4 “Desert” Results in the GOODS-N Field

While most of our effort to date on “redshift desert” galaxies has been concentrated in specially chosen fields with multiple bright background QSOs for the IGM component of the survey (not discussed here), we have also worked in fields with extensive existing or planned multi-wavelength observations. One of these fields is GOODS-N (formerly known as HDF-N). This is one of two fields in which we have targeted significant numbers of galaxies in both the $z \simeq 1.5 - 2$ and $z \simeq 2 - 2.5$ redshift range, as well as at $z \sim 3$ (see Figure 6a). The existence of large spectroscopic samples of $z > 1.4$ galaxies together with existing SCUBA, Chandra, and VLA images, as well as the very high quality GOODS/ACS images and planned SIRTf/IRAC and SIRTf/MIPS observations, will allow for a large amount of progress and a deeper understanding of the energetics, masses, and stellar populations of star forming galaxies at high redshifts. Here we make only a few comments.

There has been quite a bit of discussion about the overlap, or lack thereof, between SCUBA galaxies detected at $850 \mu\text{m}$ and the UV-selected samples of LBGs at $z \gtrsim 3$ (and now the large samples in the “redshift desert”). In fact, it turns out that there is indeed substantial overlap between the BX/BM samples and the SCUBA/radio objects of [2], and the HDF region is no exception. There are at least 4 objects in common between our BX/BM sample in GOODS-N (fig. 6a) and the radio-detected “SMGs” in the Chapman et al sample: 3 of these have LRIS-B redshifts from our own survey, at $z = 2.098$, $z = 1.989$, and $z = 1.865$. A glance at fig. 6a shows that each of these is a member of one of the redshift desert “spikes” found from the LRIS-B spectroscopic results for BX/BM galaxies, qualitatively supporting the claim (see Blain’s contributions to these proceedings) that the SMGs are strongly clustered objects. It is possible that the reason for the lack of overlap between SCUBA sources and the $z \sim 3$ LBGs may be due to the fact that the redshift distribution for SMGs peaks in the $z = 2 - 2.5$ range, very much like optically selected QSOs; $z > 3$ SMGs are relatively rare. The increase in overlap with SCUBA sources is yet another piece of evidence for significant evolution in the sample of UV-selected galaxies between $z \sim 3$ and $z \sim 2$.

Very recently we have examined the average X-ray and radio emission from the spectroscopic $z \sim 2$ galaxy sample in the GOODS-N field via a stacking analysis [12], providing a 3-way check on the average inferred star formation rate (and UV attenuation factor). The stack of the X-ray image at the positions of 160 $z \sim 2$ galaxies (after excluding all directly detected X-ray sources, among which are all 3 of the identified sub-mm/UV galaxies) in the Chandra 2 Ms image [13] is shown in fig. 6b. The stacked BX/BM galaxies are detected at

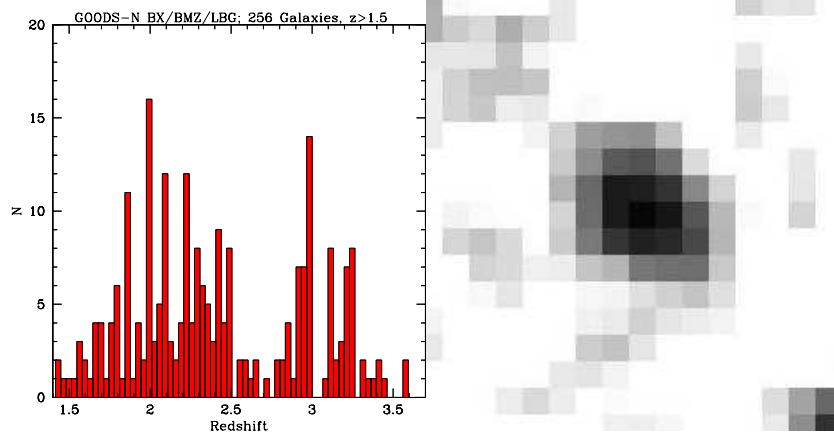


Fig. 6. **Left:** Redshift histogram of 256 $z > 1.5$ GOODS-N galaxies selected using various UV color selection techniques (those at $z < 2.6$ are based upon the BX and BM criteria). **Right:** X-ray stack of 160 $z \sim 2$ UV-selected galaxies with spectroscopic redshifts. The average X-ray flux implies an average star formation rate of $\simeq 50 M_{\odot} \text{ yr}^{-1}$, in excellent agreement with both the average SFR estimated from the radio stack and that estimated from the UV continuum slope.

the $\sim 10\sigma$ level. A similar exercise has been completed using the radio image of [14], and the estimated average star formation rate has been computed from the ground-based optical photometry assuming the [15] relation between far-UV color and far-IR luminosity. The result is that all 3 means of estimating SFR for the same sample suggest an *average* SFR of $\simeq 50 M_{\odot} \text{ yr}^{-1}$ ($h = 0.7$, $\Omega_m = 0.3$, $\Omega_{\Lambda} = 0.7$). The good agreement between UV, X-ray, and radio estimates of star formation rates suggests that, on average, the locally calibrated relationships between measurements at these wavelengths and the bolometric luminosity (i.e., SFR) still apply for starburst type systems at high redshift. The results also imply that the average $z \sim 2$ UV selected galaxy in our spectroscopic sample has a far-IR luminosity of $\langle L_{\text{bol}} \rangle \simeq 2 \times 10^{11} L_{\odot}$, which would qualify as a LIRG by the usual definition. The average implied UV extinction factor is $\simeq 5$, very much in line with the value that has been suggested for $z \sim 3$ galaxies [16][17]. With such typical luminosities, the spectroscopic $z \sim 2$ galaxies should be easily detectable by SIRTf/MIPS in the $24\mu\text{m}$ band on an individual basis (rather than by stacking a large number of objects).

5 Summary

We have highlighted the fact that, with suitable optical photometric selection and follow-up spectroscopy with a highly efficient UV/blue optimized spectrograph, the “redshift desert” ceases to exist. In fact, in many ways star forming galaxies at $z \sim 2$ offer more opportunities for measuring key physical quantities using

current generation telescopes than at any redshift beyond the local universe, because of the simultaneous access to the rest-frame far-UV and rest-frame optical spectra, and the observability of the galaxies' effects on the diffuse intergalactic medium. With the addition of high quality space-based data, particularly from SIRTf, we should learn a great deal about galaxies in this important cosmic epoch in the very near future.

We have shown that there has been significant evolution in the kinematics and the optical/IR colors of (identically) UV-selected galaxies between the epochs corresponding to $z \sim 3$ and $z \sim 2$. Both of these observations are consistent with a significant evolution (a factor of ~ 2) in the typical stellar mass of vigorously star forming systems over this redshift range. There are significant numbers of galaxies *still forming stars* at $z \sim 2$ which have already enriched themselves to solar metallicity or greater, and which have stellar masses of $\sim 10^{11} M_{\odot}$.

More quantitative results in the areas discussed above, and analyses of the clustering properties, luminosity functions, and the relationship to and interaction with the diffuse IGM are all in preparation. We would like to thank the David and Lucile Packard Foundation and the US National Science Foundation for support for this work.

References

1. C. Steidel, K. Adelberger, A. Shapley, M. Pettini, M. Dickinson, M. Giavalisco: ApJ **592**, 728 (2003)
2. S. Chapman, A. Blain, R. Ivison, I. Smail: Nature **422**, 695 (2003)
3. K. Adelberger, C. Steidel, A. Shapley, and M. Pettini: ApJ **584**, 45 (2003)
4. C. Steidel, A. Shapley, M. Pettini, K. Adelberger, D. Erb, N. Reddy, M. Hunt: ApJ in press (2004)
5. K. Adelberger, C. Steidel, A. Shapley, M. Hunt, D. Erb, N. Reddy, and M. Pettini: ApJ, in press. (2004)
6. A. Shapley, C. Steidel, K. Adelberger, M. Dickinson, and M. Giavalisco: ApJ **562**, 95 (2001)
7. D. Erb, A. Shapley, C. Steidel, M. Pettini, K. Adelberger, et al.: ApJ **591**, 101 (2003)
8. M. Pettini, Shapley, A., Steidel, C. et al: ApJ **554**, 981 (2001)
9. D. Erb, C. Steidel, A. Shapley, M. Pettini, and K. Adelberger: ApJ, submitted (2004)
10. G. Denicolo, R. Terlevich, and E. Terlevich: MNRAS **330**, 69
11. A. Shapley, et al., in preparation.
12. N. Reddy and C. Steidel: ApJL, in press (2004)
13. D. Alexander, F. Bauer, W. Brandt, et al: AJ **126**, 539 (2003)
14. E. Richards: ApJ **533**, 611 (2000)
15. G. Meurer, T. Heckman, and D. Calzetti: ApJ **521**, 64 (1999)
16. C. Steidel, K. Adelberger, M. Giavalisco, et al: ApJ **519**, 1 (1999)
17. K. Nandra, R. Mushotzky, K. Arnaud, et al: ApJ **576**, 625 (2002)